

## MODELLING SMALL AND FREQUENT AVALANCHES

Lisa Dreier\*, Yves Bühler, Walter Steinkogler, Thomas Feistl, Marc Christen, Perry Bartelt

WSL Institute for Snow and Avalanche Research SLF, Davos, Switzerland

### ABSTRACT:

Numerical simulation tools are commonly used to model extreme events, that is avalanches with return periods of 30 years or more. Recently, a new demand has arisen in avalanche engineering practice: the modelling of “small”, frequent avalanches. These avalanches with release volumes between 1,000 - 10,000 m<sup>3</sup> often threaten traffic infrastructure and ski runs. In this paper we apply a new physical avalanche model to simulate “small”, frequent avalanches using high spatial resolution DEM data. The case studies consist of avalanches documented in the Swiss accident database. For these avalanches, we have reliable data concerning release location, fracture height, run-out distance and snow temperatures at time of release. Photographs provide information regarding snow cover entrainment. A set of model parameters was determined which depends on the avalanche flow type and hence on snow temperature. We explicitly avoided changing parameters according to avalanche size. The avalanches were simulated according to the temperature classification scheme we established. We analyzed the impact of the release location, release height and entrainment on the avalanche run-out. Our results highlight the importance of release zone definition, release height, snow temperature and the difference between summer and winter terrain models for small-scale avalanches. We plan to apply the findings of this study to produce a small-scale avalanche simulation tool intended to support persons in charge of ski resorts and traffic infrastructure.

**KEYWORDS:** avalanche dynamics, avalanche mitigation, hazard assessment, snow entrainment, snow temperature.

### 1. INTRODUCTION

Land planners and engineers use numerical simulation tools for avalanche hazard studies and safety assessment. The tools have become especially useful since they predict avalanche velocity and run-out in complex three-dimensional terrain. Currently, the models are applied to simulate extreme avalanche events; that is, avalanches with large release volumes. The primary application is hazard mapping which is based on modelling avalanches with return periods of greater than (say) 30 years. Recently, however, demand has arisen to model small and frequent avalanches. Typical applications include finding the optimal location for power line masts or cable-way support pylons. Another application is to determine the optimal mix between road closure, artificial release and mitigation measures for roadways threatened by fre-

quent avalanches.

Modelling small and frequent avalanches for safety assessment presents many new problems, the least of which is the digital representation of small-scale terrain features. Aerial and terrestrial laser scanning and digital photogrammetry can provide high spatial resolution (better than 2 m) terrain models (Bühler et al. 2012). These can be smoothed (if necessary) to account for winter conditions (Maggioni et al. 2013). However, an accurate representation of small avalanche flow and run-out presents engineers with more insidious questions. These include:

- (1) How to select the location, dimension and depth of primary release zones in complex terrain (Christen et al. 2010).
- (2) How to include snow entrainment, which not only controls the avalanche mass balance, but also thermal flow regime (Maggioni et al. 2012; Steinkogler et al. 2014; Wikstroem Jones et al. 2014).
- (3) How to include important phenomena, such as secondary avalanche release, and flow deflections caused by previous avalanche deposits or road clearing.

---

\* *Corresponding author address:*

Lisa Dreier, WSL Institute for Snow and Avalanche Research SLF, Flüelastrasse 11, CH-7260 Davos Dorf, Switzerland;  
tel: +41 81 4170 261; fax: +41 81 4170 110;  
email: lisa.dreier@slf.ch

These questions were derived by Maggioni et al. (2012) and Bovet et al. (2014) after simulating several well-documented avalanches at the Italian Seehore avalanche dynamics test site. Even if the newly-developed avalanche dynamics model is capable of accurately reproducing the flow dynamics of small avalanches, it is not clear that these questions can be answered.

In this paper we selected 25 “small” avalanches with the goal of creating a consistent method to simulate “small” avalanches for hazard assessment. We concentrate on the problem of establishing temperature categories to simplify the selection of model parameters. For the selected avalanches, we have reliable data concerning release location, fracture height, run-out distance and snow temperatures at time of release. Photographs provide information regarding snow cover entrainment. To perform the numerical simulation of the avalanches we used the RAMMS extended version (Bühler et al. 2014; Christen et al. 2010).

## 2. FIELD DATA

The Swiss accident database provides the field data of the 25 avalanches in the three study areas Valais, Bernese Oberland and Davos region. We selected the avalanches from a subset of avalanches that occurred between the winter seasons 1999-2000 and 2009-2010 which Vontobel (2011) analyzed regarding terrain. For all avalanches a

mapped release area and outline were provided in addition to observed field data like release height and photos (Fig. 1).

For nine avalanches snow profiles were available to estimate the mean snow temperature of the released slab. We simulated the snow temperature with the snow cover model SNOWPACK (Lehning; Fierz 2008; Lehning et al. 1999) for 15 avalanches. Steinkogler et al. (2014) showed that SNOWPACK may be well applied to reconstruct the snow cover and its properties for past avalanches. The mean snow temperature from the snow surface to the failure layer was used as release snow temperature.

The avalanches were categorized into three flow types: dry, mixed and wet. The flow type is highly depending on snow temperatures and was determined by the measured or simulated snow temperatures. Snow temperatures below  $-4^{\circ}\text{C}$  indicate dry, snow temperatures around  $0^{\circ}\text{C}$  wet avalanche flow types. Avalanches with snow temperatures between  $-4^{\circ}\text{C}$  and  $0^{\circ}\text{C}$  could not be classified with certainty into dry or wet flow types and were categorized as mixed flow type. For seven avalanches with missing snow temperatures we estimated the flow type with the photos and the observations documented in the Swiss accident database. We identified two avalanches with a wet, 17 avalanches with a dry and six avalanches with a mixed flow type.

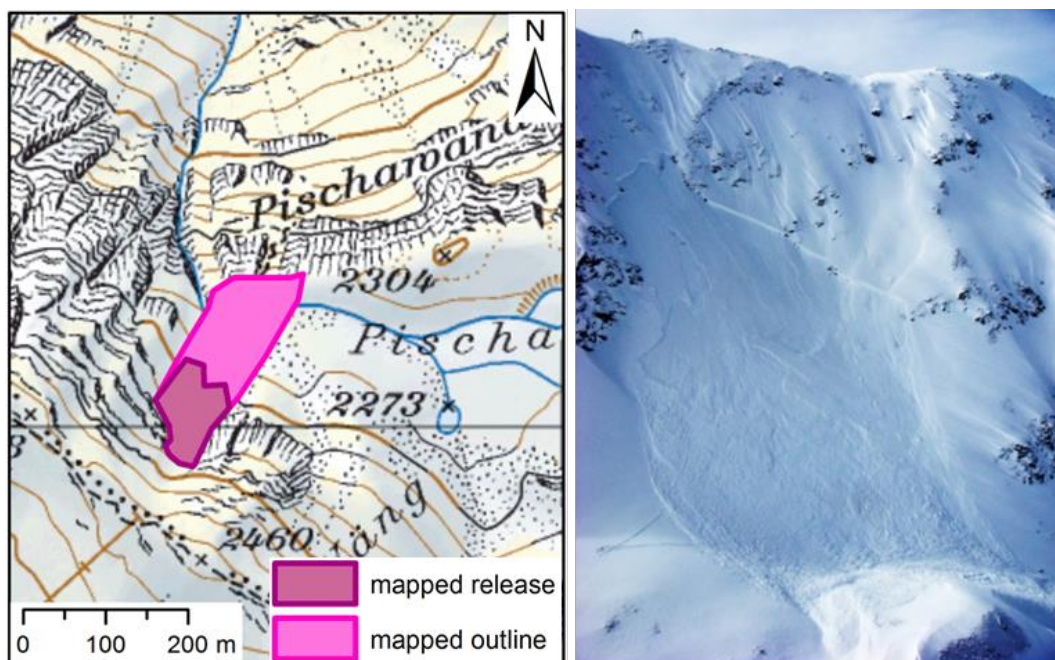


Fig. 1: Mapping and photo of avalanche #21711 at Pischa Geissrugg, Davos region (pixmaps© 2014 swisstopo (5704 000 000)).

### 3. SIMULATION MODEL AND SHEAR STRESS

The numerical simulations were performed with the RAMMS avalanche dynamics model (Christen et al. 2010). This model is based on the longstanding Voellmy shear stress formulation where the total shear resistance  $S$  is composed of the Coulomb (parameter  $\mu$ ) and turbulent (parameter  $\xi$ ) parts:

$$S = \mu N + \rho g \frac{U^2}{\xi} \quad (1)$$

where  $N$  is the total normal stress,  $\rho$  the avalanche density,  $g$  gravitational acceleration and  $U$  the mean avalanche velocity in the downslope direction. The first addend  $\mu N$  is the shear stress  $S_\mu$ .

Small avalanches are difficult to simulate with the standard Voellmy model. Therefore we applied the extended RAMMS version which accounts for streamwise density variations (Buser; Bartelt 2014), snow temperature and entrainment (Vera Valero et al. 2012). In this model the shear stress is given by

$$S_\mu = \mu N - (1 - \mu) N_0 \exp\left[-\frac{N}{N_0}\right] + (1 - \mu) N_0 \quad (2)$$

with

$$\mu = \mu_0 \exp\left[-\frac{R}{R_0}\right] \text{ and } \xi = \xi_0 \exp\left[\frac{R}{R_0}\right]. \quad (3)$$

The extended shear mode is based on the idea that when a homogeneous release slab breaks-up, it decomposes into snow fragments and granules. Because of the granular composition of the flow core, different flow configurations are possible varying from fluidized, low density, saltation like movements to dense, compact flows typical of wet snow avalanches. Fluidization is accompanied by the production of free mechanical energy associated with granule fluctuations  $R$  (Bartelt et al. 2012; Buser; Bartelt 2009). Basically, fluidized avalanches have higher  $R$ . The free mechanical energy is produced by shearing (parameter  $\alpha$ ) which depends on terrain roughness and temperature (Buser; Bartelt 2009):

$$\frac{D(Rh)}{Dt} = \alpha S U - \beta(Rh) \quad (4)$$

Granule hardness, size and density define the dissipation of  $R$  by particle interactions in the avalanche core (parameter  $\beta$ ).

The free mechanical energy is measured relative to the dense flow state. In this state the friction parameters are  $\mu_0$  and  $\xi_0$ . The activation energy  $R_0$  describes the initial energy input required to change the flow configuration and therefore the friction parameters  $\mu$  and  $\xi$ . Therefore, the primary friction parameters are no longer constant, but depend on the flow configuration of the avalanche core.

In moist snow avalanches and wet-snow avalanches, fluidization is hindered by particle cohesion (Bartelt et al. 2014). Particle cohesion is introduced by the parameter  $N_0$ , which modifies the standard linear relation between  $\mu$  and the normal stress  $N$ . Chute experiments with snow (Platzter et al. 2007) reveal a non-linear relationship which is parameterized by Eq. 2.

Snow cover entrainment is considered in RAMMS by specifying properties of the erodible snow cover including height, snow density and temperature as well as the effective entrainment rate  $\kappa$  (Christen et al. 2010).

The required input data consists of a digital elevation model (DEM) representing the three-dimensional terrain. Initial conditions are required to define the release zone location, release height and snow temperature. Friction coefficients ( $\mu_0, \xi_0$ ), cohesion  $N_0$ , activation energy  $R_0$ , energy production rate  $\alpha$  and energy decay rate  $\beta$  need to be specified as well. These parameters depend only on snow properties and do not vary as a function of avalanche size.

We used DEMs with a 2 m resolution, generated in summer season by airborne LiDAR and digital photogrammetry. The grid size of the DEM was resampled to 3 m for the simulations to obtain a smoothing effect so that the resulting DEM resembles winter terrain. We applied this method because it is simple and applicable without needing a GIS. The mapped release zones and the observed mean release heights of the Swiss accident database were used as input. Snow temperatures were set as determined (see section 2).

We analyzed the impact of the used DEM, the release zone location, release height and entrainable snow depth on the avalanche flow path and run-out.

#### 4. RESULTS AND DISCUSSION

We performed simulations for 23 of the 25 selected case studies. We used the mapped release zones for the simulations and compared the results directly to the observed avalanche outlines. This qualitative evaluation showed that the avalanches could be reproduced fitting well the mapped avalanche flow path and run-out. Most cases where we found discrepancies turned out to be due to imprecise mapping. Two avalanches could not be simulated because the mapped release zone and run-out outline could not be reproduced. Reconstructing these two events was impossible because additional photo material was lacking. The calculated release volumes of the 23 avalanches varied between 600 and 11,000 m<sup>3</sup> (Tbl. 2).

##### 4.1 *Release zone location*

The location of the release zone is critical to back-calculate the observed avalanche flow path. As demonstrated in Fig. 2, a shifting of the release zone of about 20 m can result in a different avalanche flow path than observed. In this case, the shifted release zone resulted in two avalanche flow arms instead of the observed single lobe (Fig. 3b). We had to shift the location of seven release zones (Tbl. 2). For this purpose we used photo information as a guide. In the seven events, we had to resize the zone and shift it. Twice it was necessary to shorten the release zone because it was mapped over a ridge.

From our point of view the correct mapping of release zones is crucial to simulate a realistic avalanche flow path, especially in complex terrain (Fig. 2). Good quality photos and satellite images with a high resolution are helpful to correctly map release zones for back-calculations. In real hazard studies it will be necessary to consider different scenarios with various release zone locations and sizes in order to find critical initial conditions for avalanches to reach the infrastructure. This process is different than a standard hazard mapping application, where the initial conditions are defined. In this case, we must find the most dangerous possible location and size of the release zone that endangers the object or roadway.

##### 4.2 *Summer digital elevation model (DEM)*

The numerical simulations generally worked well with the DEMs representing the summer terrain. Because the high-resolution terrain models were resampled at a resolution of 3 m, we automatically obtained a smoothing effect. Only one avalanche

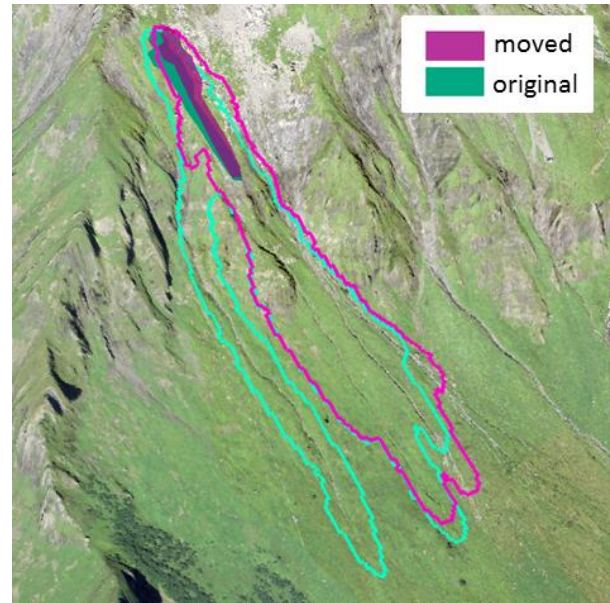


Fig. 2: Outlines of the simulation result 'Maximum flow height' for the originally mapped (green) and shifted (violet) release area location regarding the avalanche #20645 at Schilthorn, Birg (swissimage© 2014 swisstopo (DV 033594)).

was difficult to simulate with the summer DEM. This case study contained two deep gullies which constrained the flow in two flow arms. The observed avalanche in the Swiss accident database contained only one flow arm (Fig. 3).

In winter these gullies are filled with snow or deposits of previous avalanches and represent a rather smooth terrain which could not be obtained by the resampling and smoothing we applied (Fig. 3). Generally summer DEMs cannot account for variable snow accumulation due to snow drift and depositions of previous avalanches eventually deflecting the concerned avalanche (Maggioni et al. 2013). It strongly depends on the terrain and the snow conditions if a lower resolution sufficiently smoothes the terrain model and the resulting DEM resembles the winter terrain.

##### 4.3 *Simulation parameter set*

We found a useful and consistent parameter set categorized according to avalanche flow type. Tbl. 1 shows the parameter values we used for the simulations. They are based on the values which are currently used to simulate avalanches at the Vallée de la Sionne test site. Tbl. 2 shows which parameter set was selected for each avalanche. In the simulations we varied the parameter values within the range shown in Tbl. 1 in order to find the optimum values regarding avalanche flow path and run-out. The static friction coefficient  $\mu_0$  and the turbulent friction  $\xi_0$  were held quasi constant



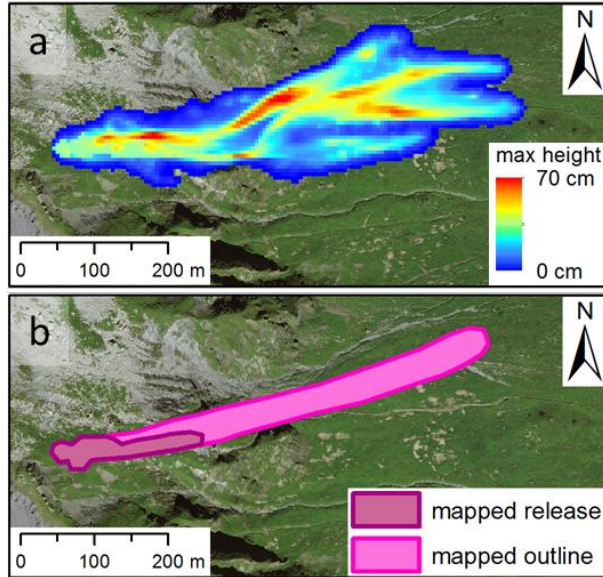


Fig. 3: (a) Simulation result 'Maximum flow height' of the avalanche #20645 at Schilthorn, Birg, with two distinct main flow arms. (b) The originally mapped avalanche outline consisting of a single flow arm (swissimage© 2014 swisstopo (DV 033594)).

with  $\mu_0$  varying between 0.50 and 0.55 and  $\xi_0$  ranging from 1500 to 1800  $\text{ms}^{-2}$  for avalanches with a wet or dry flow type respectively. Cohesion  $N_0$  increases from 0 to 300 Pa with rising snow temperature, indicating the increase of moisture in the snow pack due to wet snow granules. The ratio  $\alpha/\beta$  varied from 0.056 to 0.100 for dry and mixed flow type avalanches and amounted 0.050 for both wet flow type avalanches. For wet avalanches the energy decay rate  $\beta$  is higher in proportion to the energy production rate  $\alpha$  than for dry avalanches. The activation energy  $R_0$  varied from 2 to 3  $\text{kJm}^{-3}$  for dry and wet flow type avalanches respectively. In six cases we applied snow entrainment (Tbl. 2).

As the simulated run-out matched the mapped avalanche run-outs well, there was no need to

modify the proposed model parameters. These parameters are essentially the values now in use to model large avalanches at the Vallée de la Si-onne test site (Bartelt et al. 2012). They are close to values used by Maggioni et al. (2012) to back-calculate avalanches at the Italian Seehore test site.

#### 4.4 Release height vs Entrainment

We found that the release height influences avalanche run-out. The run-out outlines of the avalanche #21675 at Becca Colinte vary considerably for different release heights from 20 to 100 cm (Fig. 4a). In contrast mass entrainment seems to have less influence since avalanche run-outs remained similar for different maximum entrainable snow depths (see Fig. 4b). Run-outs even shortened with increasing entrainable snow depths of 20 cm, 50 cm and 100 cm despite an increase of the volume of eroded snow (2431  $\text{m}^3$ , 5014  $\text{m}^3$  and 6975  $\text{m}^3$  respectively). This is a somewhat surprising result as mass entrainment usually increases avalanche run-out. The slightly shorter run-outs for increasing snow depths are associated with decreasing maximum flow velocities. That is, the avalanche slows down as it requires energy to pick up and accelerate the entrained snow mass. This finding is in line with the results of Bartelt et al. (2012). Deposition heights in the run-out zone increase significantly from barely 60 cm without entrainment to above 2 m with entrainment (100 cm).

The run-outs of the avalanche #20634 at Vordere Bütlasse are influenced by release height though not as much as by entrainment (Fig. 4c and 4d). The volumes of eroded snow are comparable to those of the #21675 Becca Colinte avalanche and result nonetheless in much longer run-outs.

Tbl. 1: Model parameter set used for the numerical simulation of the selected avalanches. The parameter set is categorized according to avalanche flow type which depends on snow temperature  $T$ .

		Dry $T < -4 \text{ } ^\circ\text{C}$	Mixed $-4 < T < 0 \text{ } ^\circ\text{C}$	Wet $T \approx 0 \text{ } ^\circ\text{C}$
Static friction	$\mu_0$	0.55	0.55	0.50
Turbulent friction	$\xi_0$	1800 $\text{ms}^{-2}$	1500 $\text{ms}^{-2}$	1500 $\text{ms}^{-2}$
Cohesion	$N_0$	0 - 100 Pa	100 - 150 Pa	200 - 300 Pa
Energy production rate	$\alpha$	0.05 - 0.1	0.05 - 0.1	< 0.05
Energy decay rate	$\beta$	0.6 (- 0.9) $\text{s}^{-1}$	1.0 $\text{s}^{-1}$	1.0 - 1.5 $\text{s}^{-1}$
Activation energy	$R_0$	2 $\text{kJm}^{-3}$	2 - 3 $\text{kJm}^{-3}$	3 $\text{kJm}^{-3}$

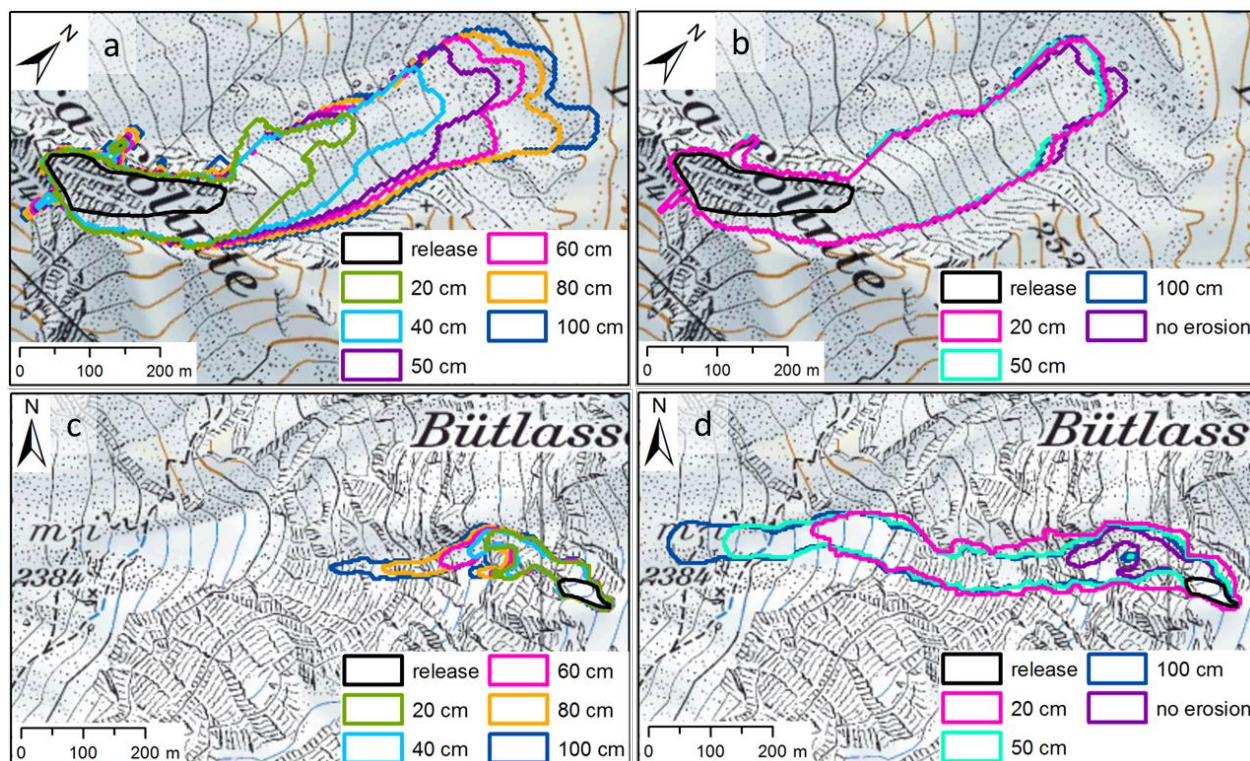


Fig. 4: Outlines of the simulation result 'Maximum flow height' of (a and b) the avalanche #21675 at Becca Colinte, Bourg-Saint-Pierre and (c and d) the avalanche #20634 at Vordere Bütlasse with (a and c) varied release heights and (b and d) varied erosion depths. When varying release heights the entrainment process was not considered. For the variation of the erosion depths parameters were set according to the observations and the found optimum. This is at Becca Colinte (b) release height = 50 cm, erosion factor  $\kappa = 0.6$  and snow temperature of entrained snow =  $-4.0\text{ }^{\circ}\text{C}$ . At Vordere Bütlasse (d) parameters were set to release height = 60 cm, erosion factor  $\kappa = 0.8$  and snow temperature of entrained snow =  $-2.0\text{ }^{\circ}\text{C}$  (pixmaps© 2014 swisstopo (5704 000 000)).

The influence of snow mass entrainment on the run-out of "small" avalanches appears to depend on the terrain. Mass entrainment does not play an important role on tracks that are short, with small drop distances and flat run-out zones. In fact, in the case of the #21675 Becca Colinte avalanche, mass entrainment appears to slow the avalanche down. The expected longer run-outs with increasing entrained snow mass were obtained in the long and steep track of the #20634 Vordere Bütlasse avalanche (Fig. 4d). In accordance with the findings of Maggioni et al. (2012) we think that snow mass entrainment influences "small" avalanches be it in form of longer run-outs or larger deposition heights. Further investigations need to be done regarding snow mass entrainment and snow temperature entrainment (Wikstroem Jones et al. 2014).

## 5. CONCLUSIONS

We simulated 23 "small" accident avalanches in the Swiss Alps and compared them to the mapped run-out outlines in the Swiss accident database. We found:

- Both release zone location and release height defined the avalanche flow path and run-out respectively.
- The resampled (i.e. smoothed) summer DEM appeared to accurately represent winter conditions, except for one case. In this case, deep gullies found in the summer DEM were probably filled with avalanche snow from previous events.
- We used a set of model parameters categorized according to avalanche flow type. Flow type is defined by snow temperature. Dry avalanches were defined to occur for temperatures  $T < -4\text{ }^{\circ}\text{C}$ ; mixed dry-wet avalanches for temperatures between  $-4\text{ }^{\circ}\text{C} < T < 0\text{ }^{\circ}\text{C}$  and wet avalanches for temperatures near zero degree. We did not vary the parameters according to avalanche size. This parameter categorization will continue to be refined and is necessary for practical application.

- The influence of snow mass entrainment on avalanche run-out appears to depend strongly on terrain i.e. the steepness and length of the avalanche path. Flat run-out zones lessen the dependency of avalanche run-out on mass entrainment, as all avalanches are strongly decelerated.

In hazard studies involving “small” and frequent avalanches it will be a challenge to define the boundary conditions such as release zone location, release height, snow temperatures and snow entrainment. Small variations in the definitions of these parameters can lead to significant differences in the calculated spatial area inundated by the avalanche. A particularly difficult problem to solve is the inclusion of avalanche deposits of previous avalanches which can fill in gullies or deflect the avalanche.

In conclusion, the primary hindrance to the application of numerical models to simulate “small” and frequent avalanches appears to be the specification of the initial and boundary conditions, not the definition of an appropriate set of model parameters. A possible method to define boundary conditions is to apply a reverse approach in which simulations are used to find the envelope of critical initial and boundary conditions that endanger a specific point in the avalanche path. The release location, release height and entrainment conditions will all differ for different avalanche flow types dry, mixed and wet. The simulation results could support authorities in charge of ski resorts and traffic infrastructure. A type of hazard map could be provided. However, based on our results, we do not believe – or recommend – that numerical simulations be used for real-time avalanche warning as the specification of initial and boundary conditions is decisive.

## ACKNOWLEDGEMENTS

We thank the WSL directorate for the funding of the internal project which made this work possible. Thank you to Frank Techel and Stephan Harvey which provided us with the data basis for this study.

## REFERENCES

- Bartelt, P., Y. Bühler, O. Buser, M. Christen, and L. Meier, 2012: Modeling mass-dependent flow regime transitions to predict the stopping and depositional behavior of snow avalanches. *Journal of Geophysical Research: Earth Surface*, **117**.
- Bartelt, P., C. Vera Valero, T. Feistl, M. Christen, Y. Bühler, and O. Buser, 2014: A model for cohesion in snow avalanche flow. *Submitted to the Journal of Glaciology*.
- Bovet, E., and Coauthors, 2014: Simulating small avalanches: A comparison to field measurements obtained at the Italian avalanche test site Seehore. *Submitted to the Journal of Glaciology*.
- Bühler, Y., M. Marty, and C. Ginzler, 2012: High resolution DEM generation in high-alpine terrain using airborne remote sensing techniques. *Transactions in GIS*, **16**, 635-647.
- Bühler, Y., M. Christen, L. Dreier, T. Feistl, and P. Bartelt, 2014: Merging of recent developments in avalanche simulation technology into practice. *This issue*.
- Buser, O., and P. Bartelt, 2009: Production and decay of random kinetic energy in granular snow avalanches. *Journal of Glaciology*, **55**, 3-12.
- Buser, O., and P. Bartelt, 2014: Modelling snow avalanches: Streamwise density variations in a granular flow. *Submitted to the Journal of Glaciology*.
- Christen, M., J. Kowalski, and P. Bartelt, 2010: RAMMS: Numerical simulation of dense snow avalanches in three-dimensional terrain. *Cold Regions Science and Technology*, **63**, 1-14.
- Lehning, M., and C. Fierz, 2008: Assessment of snow transport in avalanche terrain. *Cold Regions Science and Technology*, **51**, 240-252.
- Lehning, M., P. Bartelt, B. Brown, T. Russi, U. Stöckli, and M. Zimmerli, 1999: Snowpack model calculations for avalanche warning based upon a new network of weather and snow stations. *Cold Regions Science and Technology*, **30**, 145-157.
- Maggioni, M., M. Freppaz, M. Christen, P. Bartelt, and E. Zanini, 2012: Back-Calculation of small avalanches with the 2D avalanche dynamics model RAMMS: Four events artificially triggered at the Seehore test site in Aosta Valley (NW Italy). *International Snow Science Workshop ISSW 2012, Anchorage, Alaska, U.S.A., 16-21 September 2012*, 591-598.
- Maggioni, M., and Coauthors, 2013: Influence of summer and winter surface topography on numerical avalanche simulations. *International Snow Science Workshop ISSW 2013, Grenoble Chamonix Mont-Blanc, France, 7-11 October 2013*, 591-598.
- Platzer, K., P. Bartelt, and M. Kern, 2007: Measurements of dense snow avalanche basal shear to normal stress ratios (S/N). *Geophysical Research Letters*, **34**.
- Steinkogler, W., B. Sovilla, and M. Lehning, 2014: Influence of snow cover properties on avalanche dynamics. *Cold Regions Science and Technology*, **97**, 121-131.
- Vera Valero, C., T. Feistl, W. Steinkogler, O. Buser, and P. Bartelt, 2012: Thermal temperature in avalanche flow. *International Snow Science Workshop ISSW 2012, Anchorage, Alaska, U.S.A., 16-21 September 2012*, 32-37.
- Vontobel, I., 2011: Geländeanalysen von Unfalllawinen. Master thesis, Department of Geography, University of Zurich, 89 pp.
- Wikstroem Jones, K., D. Hamre, and P. Bartelt, 2014: Effects of the thermal characteristics of snow entrainment in avalanche run-out at Bird Hill, south-central Alaska. *This issue*.

Tbl. 2: The selected avalanches with the initial conditions calculated release volume and avalanche flow type as well as simulation results regarding avalanche run-out.

Nr.	Location	Release volume (m <sup>3</sup> )	Edited mapped release zone	Parameter set	Entrainment applied	Run-out (simulated)
20319	Cabane du Velan	10,326	-	Wet	Yes; run-out slightly longer	Second mapped lobe not reproducible
20822	Mont de l'Etoile	2,222	Remapped	Mixed	Yes; run-out slightly longer	Narrower than mapped run-out (channeling)
21176	Col de la Chaux	10,677	-	Mixed	No	Shifted flow path in simulation due to incorrect mapping
21375	Becca Colinte	3,511	Shortened length	Dry	Yes; nearly doubling flow volume, triple deposition heights	Small deviation of flow path; Mapped finger of run-out reproducible
22270	Col du Crêt	5,100	-	Mixed	No	Two mapped flow arms well reproduced
21411	La Cassorte	5,848	-	Dry	No	Mapped run-out slightly too short; Simulation fits run-out on photos
21483	Bec de la Montau	3,097	-	Dry	No	Mapped run-out slightly too short; Simulation fits run-out on photos
21485	Mont Rogneux	985	-	Dry	No	Flow path more curved than mapped outline
20634	Vordere Bütlasse	658	Resized and shifted	Mixed	Yes; Avalanche not reproducible without entrainment	Run-out slightly shorter and more curved than mapped outline
20645	Schilthorn	1,681	Shifted	Mixed	Yes; run-out much longer	Two flow arms instead of one lobe as mapped
21304	Hockenhorn	1,220	-	Dry	No	Shifted flow path in simulation compared to mapped path
21445	Ärmighnubel	2,066	-	Mixed	No	Fits well mapped run-out
21466	Schilthorn	3,883	-	Wet	No	Slightly narrower than mapped run-out
21110	Hockenhorn	-	-	Dry	-	-
22884	Gehrihore	693	Shifted	Dry	No	Mapped run-out too long; Simulation fits run-out on photos
20276	Meierhoferfälli	4,295	Shortened (mapped over ridge)	Dry	No	Fits well mapped run-out
20850	Zenjflue	627	-	Dry	No	Slightly longer and narrower than mapped run-out
21412	Salezehorn	1,542	-	Dry	No	Two lobes reproduced; Run-out slightly wider as mapped
21711	Pischa Geissrugg	2,154	-	Dry	No	Fits well mapped run-out
22588	Pischaboden	1,880	-	Dry	No	Mapped run-out too long; Simulation fits with run-out on photos
20615	Kreuzweg	-	-	Dry	-	-
21932	Meierhoferfälli	786	-	Dry	No	Slightly shifted flow path in simulation compared to mapped path
21981	Casanna	1,275	Remapped	Dry	No	Avalanche mapping incorrect; Simulation fits run-out on photos
21998	Hauptertälli	743	-	Dry	No	Mapped run-out too short; Simulation fits with run-out on photos
22242	Schwarzhorn	717	-	Dry	Yes; reduces run-out and doubles deposition heights	Fits well mapped run-out